Naunyn-Schmiedeberg's Archives of Pharmacology (2019) 392:199–208
https://doi.org/10.1007/s00210-018-1582-5

ORIGINAL ARTICLE

Hydrolysis of the non-canonical cyclic nucleotide cUMP by PDE9A: kinetics and binding mode

Jessica Scharrenbroich[1] · Volkhard Kaever[2] · Stefan Dove[3] · Roland Seifert[1] · Erich H. Schneider[1]

Received: 1 September 2018 / Accepted: 7 November 2018 / Published online: 15 November 2018

Abstract

The non-canonical cyclic nucleotide cUMP and the phosphodiesterase PDE9A both occur in neuronal cells. Using HPLC-coupled tandem mass spectrometry, we characterized the kinetics of PDE9A-mediated cUMP hydrolysis. PDE9A is a low-affinity and high-velocity enzyme for cUMP (V_{max} = ~ 6 μmol/min/mg; K_m = ~ 401 μM). The PDE9 inhibitor BAY 73-6691 inhibited PDE9A-catalyzed cUMP hydrolysis (K_i = 590 nM). Docking studies indicate two H-bonds between the cUMP uridine moiety and Gln453/Asn405 of PDE9A. By contrast, the guanosine moiety of cGMP forms three H-bonds with Gln453. cCMP is not hydrolyzed at a concentration of 3 μM, but inhibits the PDE9A-catalyzed cUMP hydrolysis at concentrations of 100 μM or more. The probable main reason is that the cytosine moiety cannot act as H-bond acceptor for Gln453. A comparison of PDE9A with PDE7A suggests that the preference of the former for cGMP and cUMP and of the latter for cAMP and cCMP is due to stabilized alternative conformations of the side chain amide of Gln453 and Gln413, respectively. This so-called glutamine switch is known to be involved in the regulation of cAMP/cGMP selectivity of some PDEs.

Keywords Cyclic UMP · Cyclic CMP · Phosphodiesterase · PDE9A · Enzyme kinetics · Glutamine switch

Abbreviations

BSA	Bovine serum albumin
cAMP	Adenosine 3′,5′-cyclic monophosphate
cCMP	Cytidine 3′,5′-cyclic monophosphate
cGMP	Guanosine 3′,5′-cyclic monophosphate
CMP	Cytidine 5′-monophosphate
cNMP	Nucleoside 3′,5′-cyclic monophosphate
cUMP	Uridine 3′,5′-cyclic monophosphate
EDTA	Ethylenediaminetetraacetic acid
ExoY	Exotoxin of *Pseudomonas aeruginosa* with nucleotidyl cyclase properties
GMP	Guanosine 5′-monophosphate
GST	Glutathione S-transferase (used as protein tag)
HCN	Hyperpolarization-activated cyclic nucleotide-gated channel
HPLC-MS/MS	High-performance liquid chromatography-coupled tandem mass spectrometry
IBMX	3-Isobutyl-1-methylxanthine
K_m	Michaelis-Menten constant
MRP	Multidrug resistance-associated protein
NMP	Nucleoside 5′-monophosphate
PDE	Phosphodiesterase
PKA	Protein kinase A
PKG	Protein kinase G
sAC	Soluble adenylyl cyclase
SD	Standard deviation
SEM	Standard error of the mean
sGC	Soluble guanylyl cyclase
UMP	Uridine 5′-monophosphate
V_{max}	Maximum velocity of an enzymatic reaction under saturating conditions

✉ Erich H. Schneider
schneider.erich@mh-hannover.de

[1] Hannover Medical School, Institute of Pharmacology, Carl-Neuberg-Str. 1, 30625 Hannover, Germany

[2] Research Core Unit Metabolomics, Hannover Medical School, Institute of Pharmacology, Carl-Neuberg-Str. 1, 30625 Hannover, Germany

[3] Department of Medicinal Chemistry II, Institute of Pharmacy, University of Regensburg, 93040 Regensburg, Germany

Introduction

While the canonical cyclic nucleotides (cNMPs) cyclic adenosine monophosphate (cAMP) and cyclic guanosine monophosphate (cGMP) are well-established second messengers, only little is known about metabolism and biological effects of the non-canonical cNMPs cyclic cytidine monophosphate (cCMP) and cyclic uridine phosphate (cUMP) (Seifert et al. 2015). With the advent of highly sensitive and specific high-performance liquid chromatography quadrupole time of flight mass spectrometry (HPLC-MS/TOF) as well as HPLC-coupled tandem mass spectrometry (HPLS-MS/MS), however, it became possible to identify and quantitate cCMP and cUMP in biological matrices (Seifert et al. 2015) and significant amounts of cCMP and cUMP have been detected in mammalian cells (Hartwig et al. 2014). Both cCMP and cUMP are mainly synthesized by the bicarbonate-dependent soluble adenylyl cyclase (sAC) (Hasan et al. 2014) as well as, to a minor degree, by soluble guanylyl cyclase (sGC), which is activated by nitric oxide (Bähre et al. 2014). Furthermore, cUMP and cCMP are generated by certain bacterial nucleotidyl cyclase toxins such as ExoY secreted by *Pseudomonas aeruginosa* (Beckert et al. 2014b). cUMP and cCMP both activate protein kinase A (PKA) and protein kinase G (PKG) in vitro (Wolter et al. 2011). Besides, they stimulate the hyperpolarization-activated cyclic nucleotide-gated channels (HCN channels) 2 and 4 to a comparable extent (Zong et al. 2012). Inactivation of cCMP and cUMP can be achieved through export via the multidrug resistance-associated proteins MRP 4 (cUMP) or MRP 5 (cCMP, cUMP) (Laue et al. 2014). Alternatively, the phosphodiesterase PDE7A is capable of hydrolyzing cCMP (Monzel et al. 2014), while PDE3A (Reinecke et al. 2011; Berrisch et al. 2017), PDE3B (Reinecke et al. 2011; Ostermeyer et al. 2018), and PDE9A (Reinecke et al. 2011) inactivate cUMP.

This article focuses on cUMP hydrolysis by PDE9A, which reportedly shows very high selectivity and nanomolar affinity for cGMP (Fisher et al. 1998). PDE9 is highly conserved across various species (van Staveren et al. 2002) and shows the highest expression levels in the brain, the kidneys and the intestinal tract (Fisher et al. 1998; Soderling et al. 1998; van Staveren et al. 2002). It is unresponsive to several PDE inhibitors such as the non-selective PDE inhibitor 3-isobutyl-1-methylxanthine (IBMX) (Soderling et al. 1998). Previous studies show that inhibition of the PDE9A with the PDE9A-specific inhibitor BAY 73-6691 enhances learning and memory in rodents (van der Staay et al. 2008), rendering PDE9A an important potential target for the treatment of Alzheimer's disease (Wunder et al. 2005).

Here, we report the basic enzyme kinetics parameters for PDE9A-mediated cUMP hydrolysis and show that the structurally closely related cCMP is not hydrolyzed by the enzyme, but inhibits PDE9A-mediated cUMP hydrolysis with low potency. Our results indicate that PDE9A is a high-velocity and low affinity enzyme for cUMP. Moreover, we postulate a binding mode for both cCMP and cUMP at the active site of PDE9A and compare it with the corresponding binding site of the recently characterized cCMP-hydrolyzing PDE7A (Monzel et al. 2014). The so-called glutamine switch seems not only to control selectivity of PDE9A for cGMP as compared to cAMP, but also regulates preference of PDE9A for cUMP over cCMP.

Materials and methods

Enzymes and reagents

Recombinant human PDE9A2 (lot # 130906-G2) was purchased from BPS Bioscience (San Diego, CA, USA). The enzyme had a purity of > 90%, was N-terminally GST tagged and exhibited a specific activity of ≥ 1050 pmol/min/μg. The cyclic nucleotides 3′-5′-cUMP, 3′-5′-cGMP and 3′-5′-cCMP were obtained from Sigma-Aldrich (Steinheim, Germany). The PDE9 specific inhibitor BAY 73-6691 (1-(2-Chlorophenyl)-6-[(2R)-3,3,3-trifluoro-2-methylpropyl]-1,5-dihydro-4H-pyrazolo[3,4-d]pyrimidine-4-one; Sigma-Aldrich, Steinheim, Germany, lot # 089K4608V) was dissolved in DMSO. Tenofovir from the National Institute of Health (NIH) AIDS Research and Reference Reagent Program was used as an internal standard. For all enzyme kinetic studies, 1 × PDE buffer complemented with 0.05% BSA was utilized. The 1 × PDE puffer contained 50 mM of Tris-HCl (pH 7.5), 8.3 mM of magnesium chloride, and 1.7 mM of EDTA.

Time course of PDE9A activity for cUMP, cGMP, and cCMP

All experiments were conducted in 1 × PDE buffer containing 0.05% BSA and 3 μM of cUMP, cGMP, or cCMP. Recombinant PDE9A was added at a final concentration of 0.5 μg/ml. All samples were run in duplicates and were incubated for a maximum of 120 min at 30 °C under continuous shaking (300 rpm, Eppendorf Thermomixer® comfort). Aliquots of 40 μl were taken at appropriate times and immediately heat-inactivated at 95 °C for 15 min. Subsequently, all samples were frozen overnight. After thawing and centrifuging (15 min at 20,800×*g* and 4 °C), 10 μl of the supernatant were diluted 1:4 with water. Then, 40 μl of tenofovir solution (100 ng/ml) were added to obtain a final volume of 80 μl. Substrates (cUMP, cGMP, or cCMP) and products (UMP, GMP, or CMP) were determined by HPLC-MS/MS as previously described (Monzel et al. 2014).

Michaelis-Menten analysis of PDE9A-mediated cUMP degradation

K_m and V_{max} values of PDE9A-mediated cUMP and cGMP hydrolysis were determined in 1 × PDE buffer supplemented with 0.05% of BSA using cUMP concentrations between 1 and 1500 μM. PDE9A was added at a final concentration of 0.125 μg/ml, yielding a final sample volume of 50 μl. For each substrate concentration, an enzyme-free negative control was run. All samples were run in duplicates and incubated for 15 min. After incubation, 40 μl aliquots were heated to 95 °C in order to inactivate the enzyme and precipitate the protein and frozen overnight. Afterwards, samples were processed and measured as described in "Time course of PDE9A activity for cUMP, cGMP and cCMP". Due to the high cUMP concentrations used in this assay, only UMP accumulation was determined.

PDE9A inhibition studies

For the inhibition of PDE9A-mediated cUMP hydrolysis, cUMP was used at a concentration of 3 μM in 1 × PDE buffer containing 0.02% DMSO and 0.05% BSA. The specific PDE9 inhibitor BAY 73-6691 was added in a concentration range between 1 nM and 10 μM. The reaction was started by adding PDE9A to yield a final concentration of 0.25 μg/ml and a final sample volume of 50 μl. All samples were run in duplicates. After an incubation time of 1 h under constant shaking (300 rpm, 30 °C), the samples were processed and measured as described in "Time course of PDE9A activity for cUMP, cGMP and cCMP". The potential inhibitory effect of cCMP on PDE9A-mediated cUMP hydrolysis was investigated in a similar way as described above for BAY 73-6691, but with concentrations ranging from 1 nM to 1 mM of cCMP. Since cCMP was dissolved in water, no DMSO was added to the samples. The effect of BAY 73-6691 on PDE9A-mediated cGMP hydrolysis was assayed using a cGMP concentration of 0.2 μM and a PDE9A concentration of 0.125 μg/ml. BAY 73-6691 was applied at concentrations between 1 nM and 100 μM. The final volume of each sample was 50 μl. All samples were incubated for 3.5 min (30 °C and 300 rpm) and run as duplicates. Processing and measurement were performed as described in "Time course of PDE9A activity for cUMP, cGMP and cCMP".

Docking studies

Docking studies were performed with the molecular modeling package SYBYLx 2.0 (Certara, L.P., St. Louis, MO, USA), based on crystal structures of the PDE9A-cGMP enzyme-substrate complex (PDB ID 3DYL) (Liu et al. 2008) and of PDE7A in complex with 3-isobutyl-1-methylxanthine (PDB ID 1ZKL) (Wang et al. 2005). cUMP and cCMP, respectively, were manually docked retaining the binding mode of the ribosylphosphate moiety in the PDE9A-cGMP structure. PDE9A-cUMP and PDE7A-cCMP models were prepared as follows: Hydrogens were added and charges were assigned (proteins and water molecules—AMBER_FF99; ligands—Gasteiger-Hueckel; metal ions M1, M2—formal charges of 2). Complexes were refined in two steps: first, minimization with fixed nucleotide using the AMBER_FF99 force field (Cornell et al. 1995). Second, subset minimization of the nucleotide and the surrounding (distance up to 6 Å) protein residues (Tripos force field (Clark et al. 1989)) In both minimization steps, the Powell conjugate gradient method with termination at a root-mean-square force of 0.05 kcal/mol × $Å^{-1}$ was applied.

Data analysis and statistics

Analysis of HPLC-MS/MS data was performed with the Analyst Software (ABSciex; Framingham, USA). The results were exported to Microsoft Excel® (Microsoft; Redmond, USA). The analyte amounts in the samples were calculated from the analyte peak areas in GraphPad Prism 6® (San Diego, CA, USA) by using calibration curves containing cUMP/UMP together with either cGMP/GMP or cCMP/CMP (0, 0.24, 0.49, 0.98, 1.95, 3.9, 7.8, 15.6, 31.3, 62.5, and 125 pmol). V_{max}, K_m, and IC_{50} values were calculated using GraphPad Prism 6® (San Diego, CA, USA) using nonlinear regression. For the evaluation of all enzyme kinetic experiments, the internal standard was excluded. Logarithmic errors were converted to linear errors by multiplication with ln10 and with the non-logarithmic mean value. The error bars in the graphs represent standard deviations (SD). However, the errors of K_m, V_{max}, and IC_{50} values are all given as standard error of the mean (SEM), since GraphPad Prism automatically calculates SEM and not SD, when fitting a curve.

Results

Characterization of cUMP hydrolysis by recombinant PDE9A

Functionality of the recombinant PDE9A was assessed in 120-min time course experiments with a saturating concentration (3 μM) of the high-affinity substrate cGMP in the presence of 0.5 μg/ml of PDE9A. Complete conversion to GMP occurred within 60 min (Fig. 1a). From the initial linear part of the hydrolysis curve (first 10 min), a V_{max} of ~ 0.25 μmol/min/mg was determined (Fig. 1a, Table 1). Due to the very low K_m value of PDE9A for cGMP, we were not able to obtain useful Michaelis-Menten kinetics data for cGMP hydrolysis. The low cGMP concentrations required rendered it difficult to detect the analyte. Moreover, educt depletion occurred even with

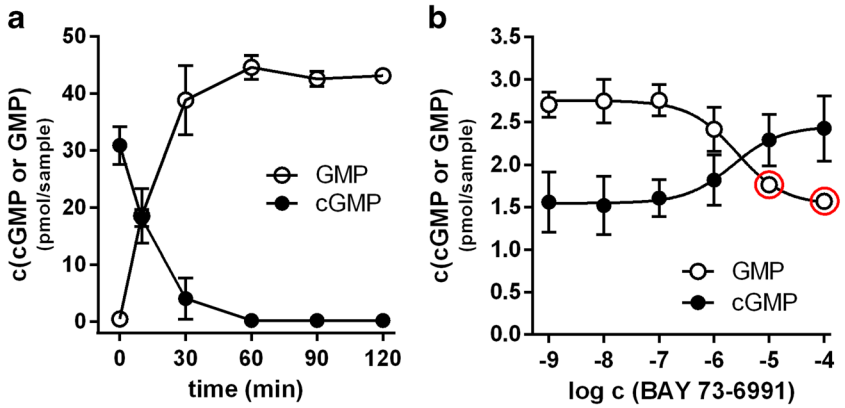

Fig. 1 Time course of PDE9A-mediated cGMP hydrolysis and inhibition by BAY 73-6991. **a** Time course of GMP generation and cGMP hydrolysis during incubation of cGMP (3 μM) with 0.5 μg/ml of PDE9A (n = 2: 90 and 120 min; n = 3: all other data points); **b** Inhibition of PDE9A-mediated cGMP hydrolysis by BAY 73-6691. The data points marked by red circles in the GMP accumulation curve were below the lower level of quantitation (LLOQ) of our HPLC-MS/MS method. Thus, the GMP accumulation curve was not used to calculate the IC_{50} and K_i values stated in the text and in Table 1. The LLOQ is defined as the lowest analyte concentration that can still be determined with an accuracy of 80–120%. Thus, the red-circled data points represent real data that may differ by more than ± 20% from the "true" value. The samples contained 0.2 μM of cGMP and 0.125 μg/ml of PDE9A (n = 3). All data are means ± SD

very low enzyme concentrations and very short incubation times (data not shown).

We also tested, whether the cGMP-hydrolytic activity in our samples is inhibited by the PDE9-selective inhibitor BAY 73-6991. In fact, BAY 73-6991 reduced hydrolysis of 3 μM of cGMP with an IC_{50} value of ~ 2.6 μM (Fig. 1b, Table 1), indicating that the observed activity is due to PDE9A. Calculation of the inhibition constant from the cGMP hydrolysis curve using the Cheng-Prusoff equation (Cheng and Prusoff 1973) and a cGMP K_m value of 70 nM (Soderling et al. 1998) yielded a BAY 73-6991 K_i value of 670 nM (Table 1). The literature cGMP K_m value of 70 nM (Soderling et al. 1998) was used for this calculation because of the aforementioned problems with determining the K_m value of PDE9A for cGMP in Michaelis-Menten kinetics experiments. We used the cGMP curve for the calculation of the K_i value, because in the GMP curve, the 10 μM and 100 μM data points were below the lower level of quantitation of our HPLC-MS/MS method (red circles in Fig. 1b).

In contrast to cGMP, cUMP was hydrolyzed by PDE9A at much slower velocity. In the presence of 0.5 μg/ml of PDE9A, more than 120 min were required to completely convert 3 μM of cUMP to the mononucleotide (Fig. 2a). To assess the basic enzyme kinetics parameters (K_m and V_{max}) for PDE9A-catalyzed cUMP hydrolysis, Michaelis-Menten experiments were conducted and the accumulation of mononucleotides was determined. The conversion of cUMP into UMP occurred with a maximum reaction velocity (V_{max}) of 6.1 ± 0.1 μmol/min/mg (Fig. 2b, Table 1). Furthermore, we determined a relatively high cUMP K_m value of 401 ± 86 μM (Fig. 2b, Table 1). These findings indicate that PDE9A is a low-affinity but high-velocity PDE for cUMP. To make sure that the observed hydrolysis of cUMP is indeed caused by PDE9A and not by an undefined contamination, we characterized the effect of the PDE9-selective inhibitor BAY 73-6691 on the hydrolysis of 3 μM of cUMP. In fact, cUMP hydrolysis was effectively inhibited by BAY 73-6691 with IC_{50} values of 594 ± 228 nM (UMP accumulation) or 329 ± 184 nM (cUMP hydrolysis) (Fig. 2c, Table 1). Using the Cheng-Prusoff equation (Cheng and Prusoff 1973) and the K_m value determined in the Michaelis-Menten kinetics, K_i values of 590 nM or 327 nM were calculated for inhibition of UMP formation or cUMP hydrolysis, respectively (Table 1).

Interestingly, even though cUMP and cCMP display a similar structure, no hydrolysis of 3 μM of cCMP occurred during 120 min of incubation with 0.5 μg/ml of PDE9A (Fig. 3a). By contrast, cUMP was readily converted to UMP in control samples (data not shown). This confirms previous findings (Reinecke et al. 2011). We investigated, whether cCMP represents a low-affinity inhibitor of PDE9A-catalyzed cUMP

Table 1 Characterization of PDE9A-mediated cUMP and cGMP hydrolysis (± SEM)

	cUMP	cGMP
K_m (μM)	401 ± 86[a]	n.d[b]
V_{max} (μmol/min/mg)	6.1 ± 0.1	0.25
IC_{50} (BAY 73–6691) (nM)	594 ± 228[a,d] 329 ± 184[c,d]	2586 ± 1093[c, d]
K_i (BAY 73–6691) (nM)	590[a] 327[c]	670[e]

[a] Calculated from the NMP formation curve

[b] n.d. = not determined

[c] Calculated from the cNMP curve

[d] Linear error calculated by multiplying the logarithmic error with ln10 and with the non-logarithmic mean value

[e] Calculated using a cGMP K_m value of 70 nM reported for PDE9 in the literature (Soderling et al. 1998)

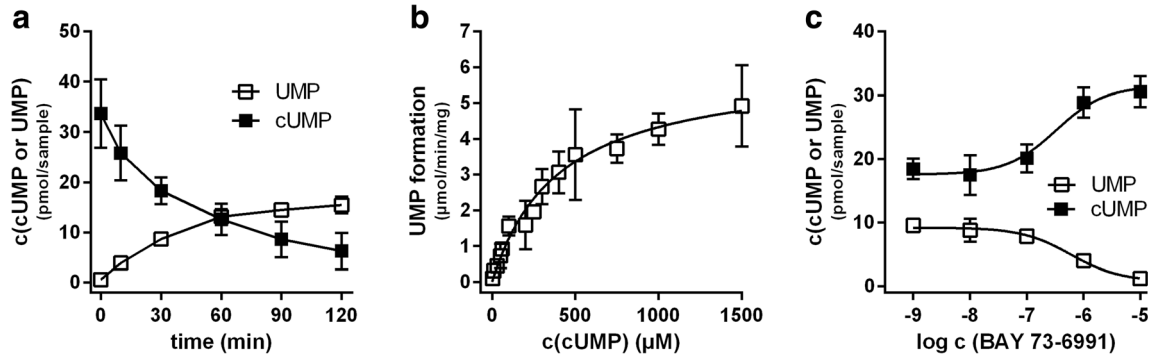

Fig. 2 Enzyme kinetic characterization of PDE9A-mediated cUMP hydrolysis. **a** Time course of cUMP degradation in presence of 0.5 μg/ml of PDE9A and 3 μM of cUMP ($n = 4$); **b** UMP formation by PDE9A (0.125 μg/ml) in the presence of cUMP (1–1500 μM) ($n = 1$: 30, 60, and 250 μM; $n = 3$: 50, 200, 300, and 400 μM; $n = 4$: all other data points); All data are means ± SD; **c** Inhibition of PDE9A-mediated cUMP hydrolysis by BAY 73-6691. The samples contained 3 μM of cUMP and 0.25 μg/ml of PDE9A ($n = 3$)

hydrolysis. In fact, a slight inhibitory effect of cCMP occurred at a concentration of 100 μM (Fig. 3b), which was further enhanced in experiments with cCMP concentrations of up to 1 mM (Fig. 3c). The data suggest a cCMP K_i value between 100 μM and 1 mM.

Binding modes and selectivity—molecular modeling studies

Essential details on cGMP binding and PDE9A catalysis became obvious from the crystal structure of the enzyme-substrate complex PDE9A-cGMP (PDB 3DYL) (Liu et al. 2008). The binding mode of cGMP corresponds to the so-called glutamine switch mechanism, originally derived from specific hydrogen bond patterns explaining substrate selectivity of PDEs 1B, 4B, 4D, and 5A (Zhang et al. 2004). The interaction between Gln453 and the adjacent Glu406 stabilizes Gln453 in a position that enables the formation of three hydrogen bonds with N1, 2-NH_2, and 6-O of the guanine base, resulting in PDE9A selectivity for cGMP (reflected, e.g., by K_m values of 0.17 μM for cGMP and 250 μM for cAMP (Liu et al. 2008)). cGMP binding is further stabilized by Phe456 and Leu420 forming a "hydrophobic clamp" that embraces the aromatic system of the guanine base. The hydrolytic center is located close to the ribosyl phosphate moiety. Two metal ions, M1 (Mn^{2+}) and M2 (Mg^{2+}), coordinate not only with adjacent amino acids and water molecules, but also with the cGMP phosphate group which is thereby activated, leading to hydrolysis of the cyclic phosphate ester by transfer of a proton from His252 onto the 3′-oxygen of cGMP.

Conserving the binding mode of the ribosyl phosphate moiety in the PDE9A-cGMP complex, cUMP can be easily docked at PDE9A without sterical clashes (Fig. 4a). The active site of the enzyme is located in a cleft between an N-terminal (residues 178–291), a central (292–361), and a C-terminal (362–505) α-helical subdomain. Metal ions M1 and M2 are coordinated with His256, His292, Asp402, and Asp293, both exocyclic phosphate oxygens and water molecules from which one, as hydroxide ion, is the nucleophile of the hydrolysis reaction (Liu et al. 2008). The ribosyl moiety contacts

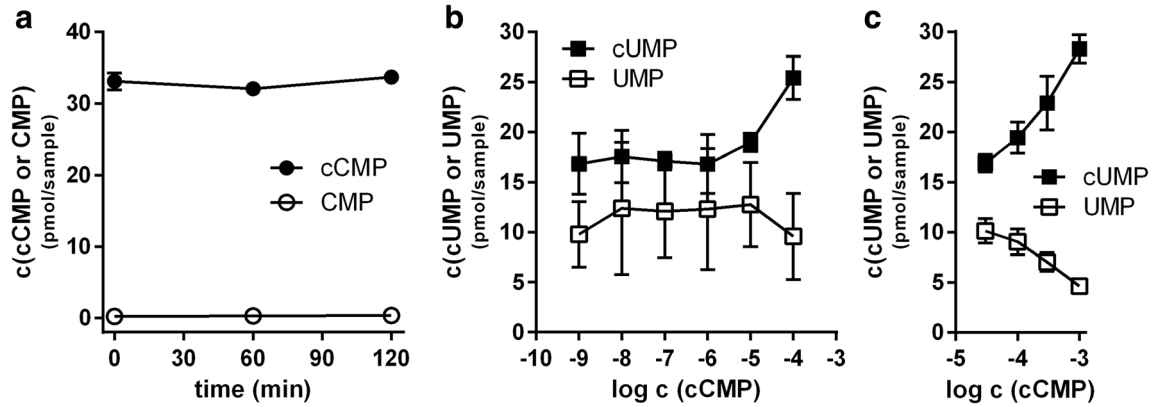

Fig. 3 Hydrolysis of cCMP by PDE9A and inhibition of PDE9A-mediated cUMP hydrolysis by cCMP. **a** Time course of cCMP hydrolysis in the presence of 0.5 μg/ml of PDE9A and 3 μM of cCMP ($n = 3$); **b** Inhibition of PDE9A-mediated cUMP hydrolysis by cCMP (cCMP concentration range 1 nM–100 μM; $n = 4$); **c** Inhibition of PDE9A-mediated cUMP hydrolysis by cCMP (cCMP concentration range 30 μM–1 mM; $n = 3$). The samples for the data shown in (**b**) and (**c**) contained 3 μM of cUMP, 0.25 μg/ml of PDE9A. All data are means ± SD

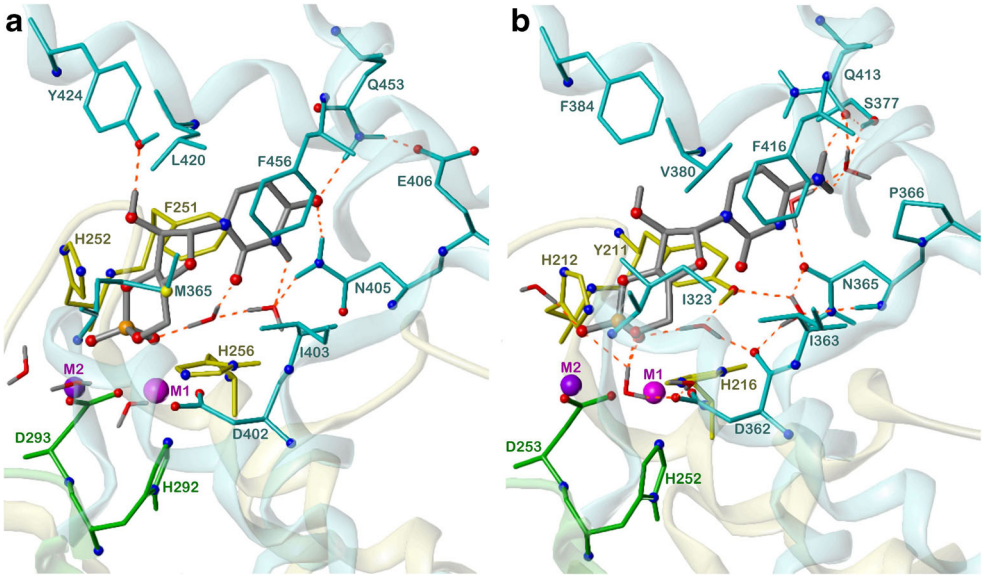

Fig. 4 Probable binding modes of **a** cUMP at PDE9A and **b** cCMP at PDE7A. Shown are all amino acids within 3.5 Å around cUMP and cCMP, respectively; atom colors N: blue; O: red; P: orange; S: yellow; M1 and M2: purple; C and polar H atoms of cUMP and cCMP: gray. C and polar H atoms as well as backbone ribbons (α-helices) and tubes are colored as per α-helical subdomains, N-terminal: yellow; central: green; C-terminal: cyan. Metal ions: M1, Mn^{2+} (PDE9A), Zn^{2+} (PDE7A); M2, Mg^{2+}. Thin sticks represent water molecules, hydrogen bonds are shown by red dashed lines

hydrophobic side chains (Met365, Ile403). O2′ and O3′ of cUMP form hydrogen bonds with Tyr424 and His252, respectively (the H252-O3′ H-bond indicates the catalytic proton transfer). Like the guanine base of cGMP, the uracil base of cUMP stacks with Phe456 on one side and contacts Phe251 and Leu420 on the other side ("hydrophobic clamp"). The 6-oxygen atom forms two hydrogen bonds with the amide NH_2 groups of Asn405 and Gln453. N3 and 2-O are involved in (putative) water-mediated hydrogen bonds.

Neither cAMP nor cCMP can bind to PDE9A like cGMP and cUMP, since the amino groups in 6- and 4-position, respectively, do not act as hydrogen bond acceptors for the Gln453 side chain amide in the given state of the glutamine switch (model not shown). In case of cAMP, affinity is reduced by more than three orders of magnitude (Liu et al. 2008). Suggesting similar K_m ratios for cGMP/cUMP and cAMP/cCMP, it is not surprising that cCMP binds only very weakly to PDE9A. By contrast, the cAMP-selective PDE7A hydrolyzes cCMP. PDE7A-mediated cUMP hydrolysis, however, occurs, if at all, at much lower velocity (Monzel et al. 2014). The PDE7A K_m value for cAMP is < 0.1 μM, but 135 μM for cCMP (Monzel et al. 2014). Similar as in the case of PDE9A, the hydrolysis rate of the non-canonical nucleotide is significantly higher than that of the canonical one (V_{max} for cAMP and cCMP hydrolysis, 0.14 and 0.56 μM/min/mg, respectively). The question arises whether cCMP may bind at PDE7A in a similar mode as cUMP at PDE9A, but with a different hydrogen bonding pattern due to the cAMP-selective state of the glutamine switch. Therefore, cCMP was docked at a crystal structure of PDE7A (PDB 1ZKL (Wang et al. 2005)) in the same conformation as that of cUMP docked at PDE9A.

The binding mode of cCMP at PDE7A is shown in Fig. 4b. The PDE binding sites of cCMP (PDE7A) and cUMP (PDE9A) are very similar (root-mean-square deviation of the backbone of all amino acids < 3.5 Å around the substrates, 0.49 Å). The ribosyl phosphates of cUMP and cCMP interact in basically the same manner with corresponding amino acids, metal ions, and a hydrolytic water molecule. Different are only the residues on both sides of the ribosyl moieties (Tyr211 and Ile323 in case of PDE7A). Furthermore, the replacement of PDE9A Tyr424 by PDE7A Phe384 does not enable a hydrogen bond of the 2′-hydroxyl. In case of PDE7A, the "hydrophobic clamp" around the cytosine base is formed by Val380 and Phe416.

PDE9A Glu406 stabilizing the cGMP-selective state of the glutamine switch is replaced by PDE7A Pro366. Instead of that, the hydroxyl of PDE7A S377 stabilizes a cAMP-selective state by a hydrogen bond with the side chain oxygen of Gln413 (Wang et al. 2005). The 6-NH_2 group of cAMP and the 4-NH_2 group of cCMP act as hydrogen bond donors for this amide oxygen. The corresponding 6-O and 4-O atoms of cGMP and cUMP, respectively, would lead to electrostatic repulsion (model not shown). Similar as in the PDE9A-cUMP complex, a specific (putative) water-mediated network of hydrogen bonds may contribute to cCMP binding at PDE7A, including the 4-NH_2 group, the side chains of Gln413, Tyr211 and Asn365, backbone atoms of Asp362 and Asn365 as well as an exocyclic phosphate oxygen. An overview of the interactions between cNMPs and key amino acids of PDE7A and 9A is given in Tables 2 and 3, respectively.

Discussion

A detailed analysis of the basic enzyme kinetic parameters of PDE9A-mediated cUMP hydrolysis is presented. Michaelis-Menten kinetics experiments revealed that PDE9A hydrolyzes

Table 2 Binding mode of cAMP, cGMP, cCMP, and cUMP to PDE7A

Hydrolytic center and catalytic mechanism[a]	Glutamine switch[b] and H-bond networks	Hydrophobic clamp[a]
M1 (Mn^{2+}) and M2 (Mg^{2+}) coordinate with His216, His252, Asp253, and Asp362, both exocyclic phosphate oxygens and H_2O molecules; the catalytic H_2O molecule donates OH^- for hydrolysis; His212 transfers H^+ onto O3' of cNMP Ribosyl moiety contacts Tyr211, Ile323; H-bonds: O3′ with His212 (initialises proton transfer); O2′ without H-bond (Tyr424 of PDE9A replaced by Phe384)	cAMP: 6-NH_2 and N1 two H-bonds with amide oxygen and NH_2, respectively, of Gln 413[c] cCMP: 4-NH_2 H-bond with amide oxygen of Gln413[c] cGMP: 6-O no H-bond with Gln413, but electrostatic repulsion; NH1 possibly H-bond with amide oxygen of Gln413 (cAMP-mode assumed) cUMP: 4-O no H-bond to Gln413, but electrostatic repulsion (cAMP-mode assumed)	One side: Phe416 Other side: Val380 Additional van der Waals contacts with Tyr211 and Ile363

[a] The interactions at the hydrolytic center, the catalytic mechanism and the hydrophobic clamp are applicable to cAMP, cGMP, cCMP and cUMP

[b] Glutamine switch of PDE7A: Gln413 stabilized in "cAMP mode" by H-bond of S377-OH with side chain oxygen of Gln413, Pro366 replaces Glu406 of PDE9A

[c] 6-NH_2 of A and 4-NH_2 of C possibly involved in H_2O-mediated H-bond network including Asn365, Gln413, Asp362, and Tyr211, exocyclic phosphate oxygen

cUMP about 24-fold faster than cGMP under saturating conditions (cUMP: $V_{max} = 6.1 \pm 0.1$ μmol/min/mg; cGMP: $V_{max} = 0.25$ μmol/min/mg). Also, PDE9A exhibits largely different K_m values for cUMP and cGMP. According to the literature, the K_m value for cGMP is as low as 0.07 μM (Soderling et al. 1998), while our Michaelis-Menten kinetic experiments resulted in a K_m value of 401 ± 86 μM for cUMP. Thus, the affinity of PDE9A for cGMP is approximately 5700-fold higher than for cUMP. This large difference may also be due to a much faster product dissociation of UMP from the active center of the enzyme compared to GMP. Taken together, PDE9A is a low-affinity and high-velocity enzyme for cUMP, similar to the other previously described cUMP-hydrolyzing PDEs 3A (Berrisch et al. 2017) and 3B (Ostermeyer et al. 2018).

The observed cUMP degradation was not caused by undefined contaminations in the enzyme preparation. First, the purity of our enzyme was ≥ 90% (according to the manufacturer's specifications) and second, the competitive PDE9A-selective inhibitor BAY 73-6691 (Wunder et al. 2005) effectively inhibited both cUMP and cGMP hydrolysis in our samples with comparable K_i values. This indicates that PDE9A in fact caused the observed cUMP hydrolysis. Surprisingly, however, although the K_i values of BAY 73-6691-mediated inhibition of PDE9A activity are similar for cUMP and cGMP in our experiments, they are 7- to 15-fold higher than the PDE9 affinity originally reported for BAY 73-6691 (Wunder et al. 2005). Since similar results were obtained with independently prepared stock solutions, we can exclude dilution errors. Our experimental conditions differed from those used by Wunder et al. (2005) in several aspects. First, our experiments were carried out with a purified GST-tagged enzyme, while a crude preparation of PDE9A-expressing Sf9 insect cells was used by Wunder et al. (2005). Second, while Wunder et al. (2005) used a [^{3}H]cGMP scintillation proximity assay to determine enzyme inhibition, our results were obtained through HPLC-MS/MS analysis. Finally, the previous literature data were obtained after incubation at room temperature (Wunder et al. 2005), while our experiments were carried out at 30 °C. We can only speculate that these and other yet undefined differences might have led to the observed discrepancy.

Table 3 Binding mode of cAMP, cGMP, cCMP, and cUMP to PDE9A

Hydrolytic center and catalytic mechanism[a]	Glutamine switch[b] and H-bond networks	Hydrophobic clamp
M1 (Mn^{2+}) and M2 (Mg^{2+}) coordinate with His256, His292, Asp293, Asp402, both exocyclic phosphate oxygens and H_2O molecules; the catalytic H_2O donates OH^- for hydrolysis; His252 transfers H^+ onto O3′ of cNMP Ribosyl moiety contacts Met365, Ile403; H-bonds: O2′ with Tyr424; O3′ with His252 (initialises proton transfer)	cGMP: NH1, 2-NH_2 and 6-O three H-bonds with Gln453 cUMP: 6-O two H-bonds with amides of Asn405 and Gln453; 2-O, N3 putative H_2O-mediated H-bonds with Asn405. cAMP: 6-NH_2 no H-bonds with Gln453 (cGMP mode assumed) cCMP: 4-NH_2 no H-bonds with Gln453 (cGMP mode assumed)	One side: Phe456 Other side: Leu420 Additional van der Waals contacts with Phe251 and Ile403

[a] The interactions at the hydrolytic center, the catalytic mechanism, and the hydrophobic clamp are applicable to cAMP, cGMP, cCMP, and cUMP

[b] Glutamine switch of PDE9A: Gln453 stabilized in "cGMP mode" by interaction with adjacent Glu406

Docking studies were performed to explore the molecular basis for the different PDE9A affinities of cUMP and cGMP. The guanine base (N1, 2-NH_2 and 6-O) of cGMP forms three direct hydrogen bonds with Gln453 which is stabilized in the appropriate glutamine switch state by Glu406. In case of cUMP, only the 4-oxygen is involved in two direct hydrogen bonds with Gln453 and Asn405. Probably, this is one of the reasons for the much higher K_m value of cUMP as compared to cGMP. Additionally, a closer fit of the larger guanine base to the "hydrophobic clamp" and a better filling of the binding site may contribute to the high cGMP affinity. Weaker PDE9A-cUMP/UMP interactions lead to fast dissociation of the product UMP as main reason for the high V_{max} value of cUMP. Nevertheless, the catalytic efficiency of PDE9A expressed by V_{max}/K_m is about 200-times higher for cGMP vs. cUMP.

Unexpectedly, cCMP was not hydrolyzed by PDE9A, but inhibited cUMP hydrolysis at concentrations > 100 μM. The concentration-effect curve indicates a K_i value between 400 μM and 1 mM. In the past, we have already described selectivity for cUMP as compared to cCMP for the dual-specific PDEs 3A and 3B (Reinecke et al. 2011; Ostermeyer et al. 2018). Although structures of PDEs 4D and 10A in complex with cAMP and cGMP provide evidence that the glutamine switch is not a common mechanism for recognition and differentiation of PDE substrates (Wang et al. 2007a; Wang et al. 2007b), PDE9A seems to be one of the PDEs with a functional glutamine switch, reasoning why cGMP and cUMP may form essential hydrogen bonds with Gln453 in contrast to cAMP and cCMP. By contrast, the cAMP-selective PDE7A contains the reversed state of the glutamine switch (Wang et al. 2005). The side chain amide of Gln413 is stabilized by Ser377 in a conformation enabling hydrogen bonds with the amino groups of cAMP and cCMP, but not with the corresponding oxygens of cGMP and cUMP. Comparing PDE9A with PDE7A (Wang et al. 2005), not only cNMP docking, but also similar orders of magnitude of V_{max} and K_m values for cGMP vs. cAMP and cUMP vs. cCMP as well as virtual inactivity for cCMP and cUMP, respectively, indicate a common catalytic mechanism, a uniform binding mode of cNMPs and a single conserved glutamine as selectivity switch. Since cCMP is virtually resistant to PDE9A-mediated hydrolysis, it might have a similar regulatory function for PDE9 as cGMP for the PDE3 isoforms 3A and 3B. PDE 3A and 3B hydrolyze cGMP and cAMP with nanomolar K_m values, but the V_{max} for cGMP is considerably slower than for cAMP (Bender and Beavo 2006). Therefore, the PDE3 isoforms are considered "cGMP-inhibited cAMP-hydrolyzing PDEs". In a similar way, PDE9A may be regarded a "low-affinity cCMP-inhibited cUMP-hydrolyzing PDE".

It is intriguing to speculate that cUMP is biologically active in the CNS and inactivated by PDE9A. Moreover, cCMP may represent a physiological PDE9A inhibitor. In fact, CNS-derived cells like B103 rat neuroblastoma cells as well as primary rat astrocytes contain almost 3-fold as much cUMP as cGMP (Hartwig et al. 2014). Furthermore, soluble adenylyl cyclase (sAC), a major source of cUMP in B103 cells (Hasan et al. 2014), is present in neurons (Chen et al. 2013) and astrocytes (Choi et al. 2012). The membrane-permeable cUMP analogue cUMP-AM (acetoxymethylester) causes aggregation of B103 cells and a round cell phenotype with neurite outgrowth (Beckert et al. 2014a). Intracerebroventricular (i.c.v.) administration of cUMP in a rat model reduces exploratory activity and body temperature and increases arterial blood pressure (Brus et al. 1984). Finally, more than 50 years ago, an undefined cUMP degrading PDE activity was reported for rabbit brain cortex (Drummond and Perrott-Yee 1961) and for rat brain (Cheung 1967), which might represent PDE9 activity.

Due to the low PDE9A affinity of cUMP and cCMP, however, a role of PDE9 and cCMP in the regulation of cUMP function would require high local concentrations of these cNMPs. It cannot be excluded that such concentrations are reached. For example, one million HEK293 cells contain 32.6 pmol of cCMP and 54.9 pmol of cUMP (Hartwig et al. 2014). Assuming a cell volume of ~ 1000 fL for a HEK293 cell (Vecsler et al. 2013), one million HEK293 cells fill a volume of about 1 μl. This results in bulk cCMP- and cUMP concentrations of 32.6 and 54.9 μM, respectively. For NO-stimulated rat cerebellar astrocytes even an intracellular cGMP concentration of ~ 800 μM was estimated in the literature (Bellamy and Garthwaite 2001). Such high cNMP concentrations could be additionally increased in intracellular microdomains containing PDE9A in spatial proximity to nucleotidyl cyclases.

PDE activity in a living cell is the net result of an interaction with various competing cNMPs rather than a reaction with just the "main substrate". In this scenario, cNMPs with low affinity for PDE9A, e.g., cAMP, cCMP, or cUMP, may increase the apparent K_m of cGMP to values much higher than the extremely low in vitro K_m values reported in the literature. Moreover, the type of cNMP hydrolyzed by a certain PDE may be cell-type dependent, because specific cell types show characteristic cNMP profiles (Hartwig et al. 2014). In fact, the "cAMP-specific" PDE4 was postulated to significantly contribute to cGMP hydrolysis in rat cerebellar astrocytes (Bellamy and Garthwaite 2001). Future studies should therefore address PDE9A enzyme activity in cNMP mixtures and compare the activity of PDE9 and other PDEs across various cell types with differing cNMP profiles. Most importantly, however, intracellular fluorescent sensors for cUMP and cCMP are urgently needed to investigate the concentrations and the fate of these "exotic" cyclic nucleotides in living intact cells.

Finally, a potential pathophysiological role of cUMP should be considered. The *Pseudomonas aeruginosa* bacterial

exotoxin and nucleotidyl cyclase ExoY preferentially generates cUMP in mammalian cells (Beckert et al. 2014b). Also, intratracheal infection of mice with an ExoY-overexpressing *P. aeruginosa* laboratory strain resulted in increased cUMP concentrations in the lung, serum, urine, and feces (Bähre et al. 2015). In this situation, cUMP-hydrolyzing low-affinity and high-velocity PDEs could represent an efficient mechanism to detoxify large amounts of cUMP. This mechanism might be additionally complemented by the multidrug resistance-associated proteins MRP 4 and MRP 5 that had previously been shown to export cUMP out of the cell (Laue et al. 2014).

However, it should also be noted that several naturally occurring *P. aeruginosa* strains express much lower amounts of the toxin (Munder et al. 2018). Nevertheless, the ExoY$^+$ *P. aeruginosa* infection model could help to clarify to which extent the expression patterns of cUMP-hydrolyzing PDEs differentially influence cUMP concentrations in various organs of the infected mice. Ideally, such experiments would require the use of PDE knockout mice as controls.

Acknowledgements We thank Prof. Dr. Martin Stangel (Dept. of Clinical Neuroimmunology and Neurochemistry, MHH) and Dr. Sabine Wolter (Institute of Pharmacology, MHH) for the excellent scientific discussions as well as Mrs. Annette Garbe (Research Core Unit Metabolomics, MHH) for the outstanding technical support.

Author contributions Participated in research design: Schneider, Scharrenbroich, Seifert
Conducted experiments: Scharrenbroich, Kaever
Performed data analysis: Scharrenbroich, Schneider
Performed docking approaches: Dove
Wrote or contributed to the writing of the manuscript: Scharrenbroich, Schneider, Dove, Kaever, Seifert

References

Beckert U, Grundmann M, Wolter S, Schwede F, Rehmann H, Kaever V, Kostenis E, Seifert R (2014a) cNMP-AMs mimic and dissect bacterial nucleotidyl cyclase toxin effects. Biochem Biophys Res Commun 451:497–502

Beckert U, Wolter S, Hartwig C, Bähre H, Kaever V, Ladant D, Frank DW, Seifert R (2014b) ExoY from Pseudomonas aeruginosa is a nucleotidyl cyclase with preference for cGMP and cUMP formation. Biochem Biophys Res Commun 450:870–874

Bellamy TC, Garthwaite J (2001) "cAMP-specific" phosphodiesterase contributes to cGMP degradation in cerebellar cells exposed to nitric oxide. Mol Pharmacol 59:54–61

Bender AT, Beavo JA (2006) Cyclic nucleotide phosphodiesterases: molecular regulation to clinical use. Pharmacol Rev 58:488–520

Berrisch S, Ostermeyer J, Kaever V, Kälble S, Hilfiker-Kleiner D, Seifert R, Schneider EH (2017) cUMP hydrolysis by PDE3A. Naunyn Schmiedeberg's Arch Pharmacol 390:269–280

Brus R, Herman ZS, Juraszczyk Z, Krzemiński T, Trzeciak H, Kurcok A (1984) Central action of cyclic: 3′,5′-thymidine, 3′,5′-uridine and 3′,5′-citidine monophosphates in rat. Acta Med Pol 25:1–9

Bähre H, Danker KY, Stasch JP, Kaever V, Seifert R (2014) Nucleotidyl cyclase activity of soluble guanylyl cyclase in intact cells. Biochem Biophys Res Commun 443:1195–1199

Bähre H, Hartwig C, Munder A, Wolter S, Stelzer T, Schirmer B, Beckert U, Frank DW, Tümmler B, Kaever V, Seifert R (2015) cCMP and cUMP occur in vivo. Biochem Biophys Res Commun 460:909–914

Chen J, Martinez J, Milner TA, Buck J, Levin LR (2013) Neuronal expression of soluble adenylyl cyclase in the mammalian brain. Brain Res 1518(1–8):1–8

Cheng Y, Prusoff WH (1973) Relationship between the inhibition constant (K1) and the concentration of inhibitor which causes 50 per cent inhibition (I50) of an enzymatic reaction. Biochem Pharmacol 22:3099–3108

Cheung WY (1967) Properties of cyclic 3′,5′-nucleotide phosphodiesterase from rat brain. Biochemistry 6:1079–1087

Choi HB, Gordon GR, Zhou N, Tai C, Rungta RL, Martinez J, Milner TA, Ryu JK, McLarnon JG, Tresguerres M, Levin LR, Buck J, MacVicar BA (2012) Metabolic communication between astrocytes and neurons via bicarbonate-responsive soluble adenylyl cyclase. Neuron 75:1094–1104

Clark M, Cramer RDI, Van Opdenbosch N (1989) Validation of the general purpose tripos 5.2 force field. J Comput Chem 10:982–1012

Cornell WD, Cieplak P, Bayly CI, Gould IR, Merz KM, Ferguson DM, Spellmeyer DC, Fox T, Caldwell JW, Kollman PA (1995) A second generation force field for the simulation of proteins, nucleic acids, and organic molecules. J Am Chem Soc 117:5179–5197

Drummond GI, Perrott-Yee S (1961) Enzymatic hydrolysis of adenosine 3′,5′-phosphoric acid. J Biol Chem 236:1126–1129

Fisher DA, Smith JF, Pillar JS, St Denis SH, Cheng JB (1998) Isolation and characterization of PDE9A, a novel human cGMP-specific phosphodiesterase. J Biol Chem 273:15559–15564

Hartwig C, Bähre H, Wolter S, Beckert U, Kaever V, Seifert R (2014) cAMP, cGMP, cCMP and cUMP concentrations across the tree of life: high cCMP and cUMP levels in astrocytes. Neurosci Lett 579:183–187

Hasan A, Danker KY, Wolter S, Bähre H, Kaever V, Seifert R (2014) Soluble adenylyl cyclase accounts for high basal cCMP and cUMP concentrations in HEK293 and B103 cells. Biochem Biophys Res Commun 448:236–240

Laue S, Winterhoff M, Kaever V, van den Heuvel JJ, Russel FG, Seifert R (2014) cCMP is a substrate for MRP5. Naunyn Schmiedeberg's Arch Pharmacol 387:893–895

Liu S, Mansour MN, Dillman KS, Perez JR, Danley DE, Aeed PA, Simons SP, Lemotte PK, Menniti FS (2008) Structural basis for the catalytic mechanism of human phosphodiesterase 9. Proc Natl Acad Sci U S A 105:13309–13314

Monzel M, Kuhn M, Bähre H, Seifert R, Schneider EH (2014) PDE7A1 hydrolyzes cCMP. FEBS Lett 588:3469–3474

Munder A, Rothschuh J, Schirmer B, Klockgether J, Kaever V, Tümmler B, Seifert R, Kloth C (2018) The Pseudomonas aeruginosa ExoY phenotype of high-copy-number recombinants is not detectable in natural isolates. Open Biol 8:170250

Ostermeyer J, Golly F, Kaever V, Dove S, Seifert R, Schneider EH (2018) cUMP hydrolysis by PDE3B. Naunyn Schmiedebergs Arch Pharmacol 391:891–905. https://doi.org/10.1007/s00210-00018-01512-00216

Reinecke D, Burhenne H, Sandner P, Kaever V, Seifert R (2011) Human cyclic nucleotide phosphodiesterases possess a much broader substrate-specificity than previously appreciated. FEBS Lett 585:3259–3262

Seifert R, Schneider EH, Bähre H (2015) From canonical to non-canonical cyclic nucleotides as second messengers: pharmacological implications. Pharmacol Ther 148:154–184

Soderling SH, Bayuga SJ, Beavo JA (1998) Identification and characterization of a novel family of cyclic nucleotide phosphodiesterases. J Biol Chem 273:15553–15558

van der Staay FJ, Rutten K, Bärfacker L, Devry J, Erb C, Heckroth H, Karthaus D, Tersteegen A, van Kampen M, Blokland A, Prickaerts J, Reymann KG, Schröder UH, Hendrix M (2008) The novel selective PDE9 inhibitor BAY 73-6691 improves learning and memory in rodents. Neuropharmacology 55:908–918

van Staveren WC, Glick J, Markerink-van Ittersum M, Shimizu M, Beavo JA, Steinbusch HW, de Vente J (2002) Cloning and localization of the cGMP-specific phosphodiesterase type 9 in the rat brain. J Neurocytol 31:729–741

Vecsler M, Lazar I, Tzur A (2013) Using standard optical flow cytometry for synchronizing proliferating cells in the G1 phase. PLoS One 8: e83935

Wang H, Liu Y, Chen Y, Robinson H, Ke H (2005) Multiple elements jointly determine inhibitor selectivity of cyclic nucleotide phosphodiesterases 4 and 7. J Biol Chem 280:30949–30955

Wang H, Liu Y, Hou J, Zheng M, Robinson H, Ke H (2007a) Structural insight into substrate specificity of phosphodiesterase 10. Proc Natl Acad Sci U S A 104:5782–5787

Wang H, Robinson H, Ke H (2007b) The molecular basis for different recognition of substrates by phosphodiesterase families 4 and 10. J Mol Biol 371:302–307

Wolter S, Golombek M, Seifert R (2011) Differential activation of cAMP- and cGMP-dependent protein kinases by cyclic purine and pyrimidine nucleotides. Biochem Biophys Res Commun 415:563–566

Wunder F, Tersteegen A, Rebmann A, Erb C, Fahrig T, Hendrix M (2005) Characterization of the first potent and selective PDE9 inhibitor using a cGMP reporter cell line. Mol Pharmacol 68:1775–1781

Zhang KY, Card GL, Suzuki Y, Artis DR, Fong D, Gillette S, Hsieh D, Neiman J, West BL, Zhang C, Milburn MV, Kim SH, Schlessinger J, Bollag G (2004) A glutamine switch mechanism for nucleotide selectivity by phosphodiesterases. Mol Cell 15:279–286

Zong X, Krause S, Chen CC, Krüger J, Gruner C, Cao-Ehlker X, Fenske S, Wahl-Schott C, Biel M (2012) Regulation of hyperpolarization-activated cyclic nucleotide-gated (HCN) channel activity by cCMP. J Biol Chem 287:26506–26512